

Supplementary material

**Potassium-ion storage behavior of microstructure-
engineered hard carbons**

*Hoseong Kim, Jong Chan Hyun, Ji In Jung, Jin Bae Lee, Jaewon Choi, Se Youn Cho,
Hyoung-Joon Jin*, and Young Soo Yun**

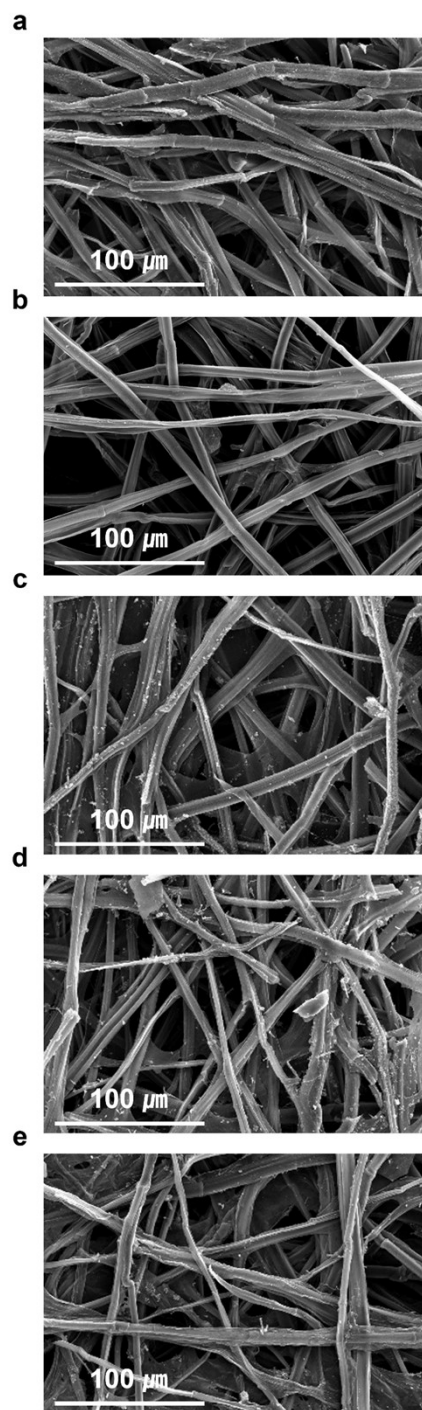


Figure S1. Morphologies of (a) DGC-1200, (b) DGC-1600, (c) DGC-2000, (d) DGC-2400, and (e) DGC-2800.

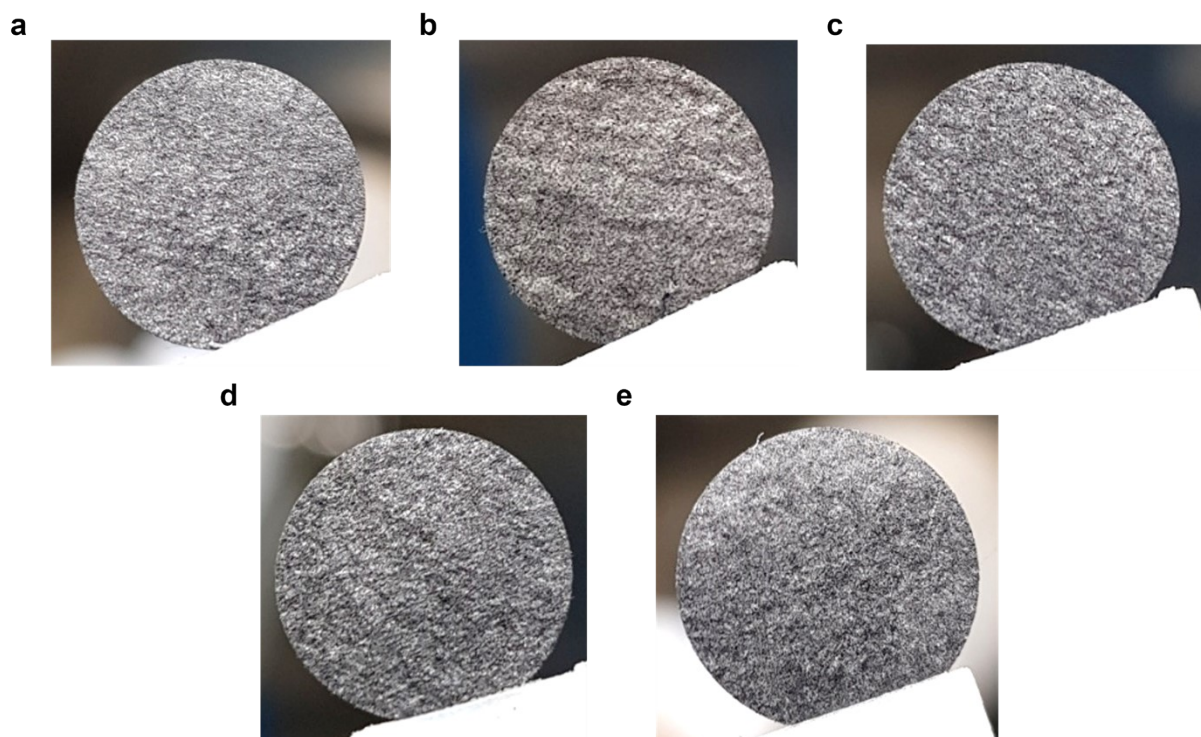


Figure S2. Optical images of the free-standing DGC electrodes: (a) DGC-1200, (b) DGC-1600, (c) DGC-2000, (d) DGC-2400, and (e) DGC-2800. All electrodes have the same size of 1/2 inch in diameter.

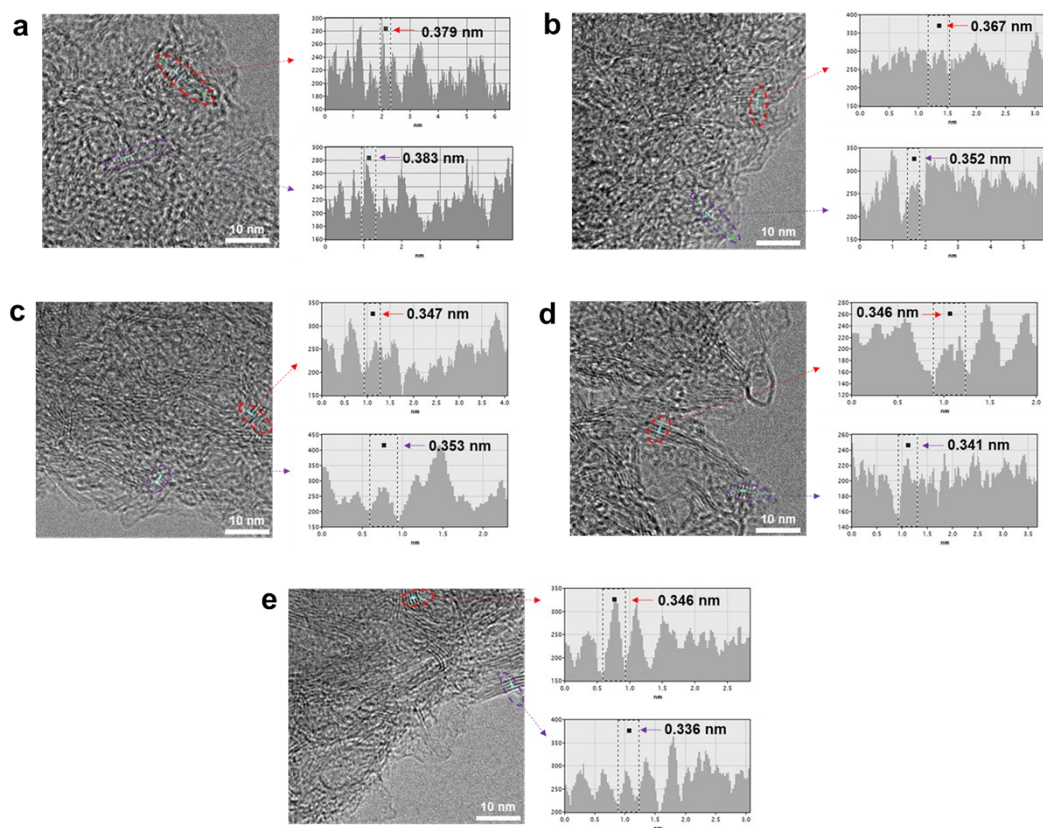


Figure S3. HRTEM images of (a) DGC-1200, (b) DGC-1600, (c) DGC-2000, (d) DGC-2400, and (e) DGC-2800 including d-spacing information at different graphitic lattices.

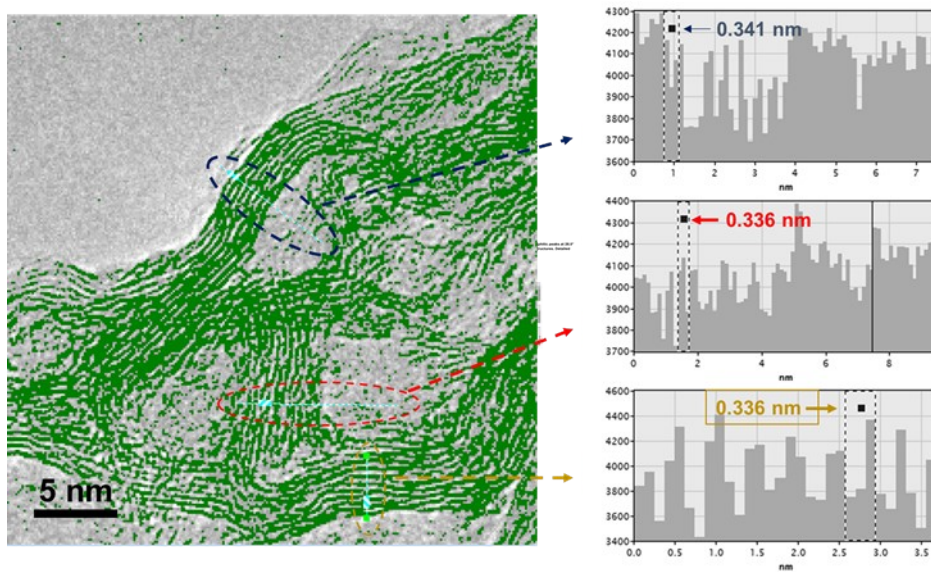


Figure S4. HRTEM image of DGC-2800 including *d*-spacing information at local graphitic lattices.

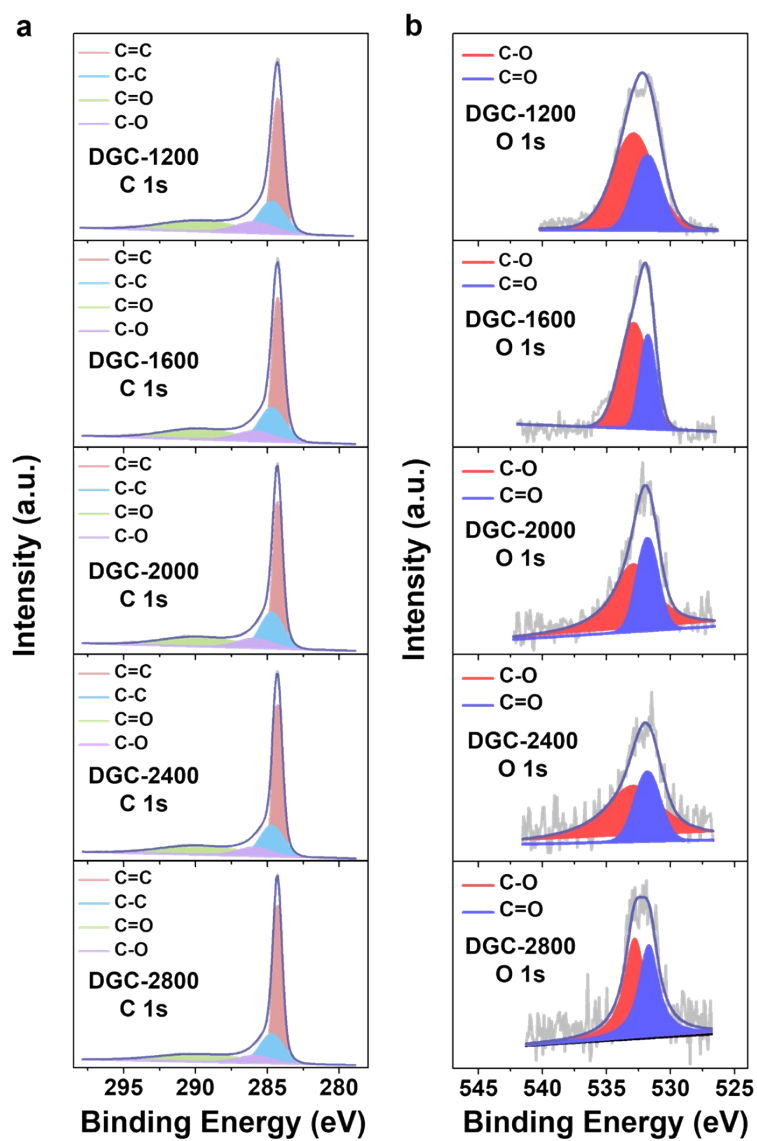


Figure S5. XPS (a) C 1s and (b) O 1s spectra of the DGC samples.

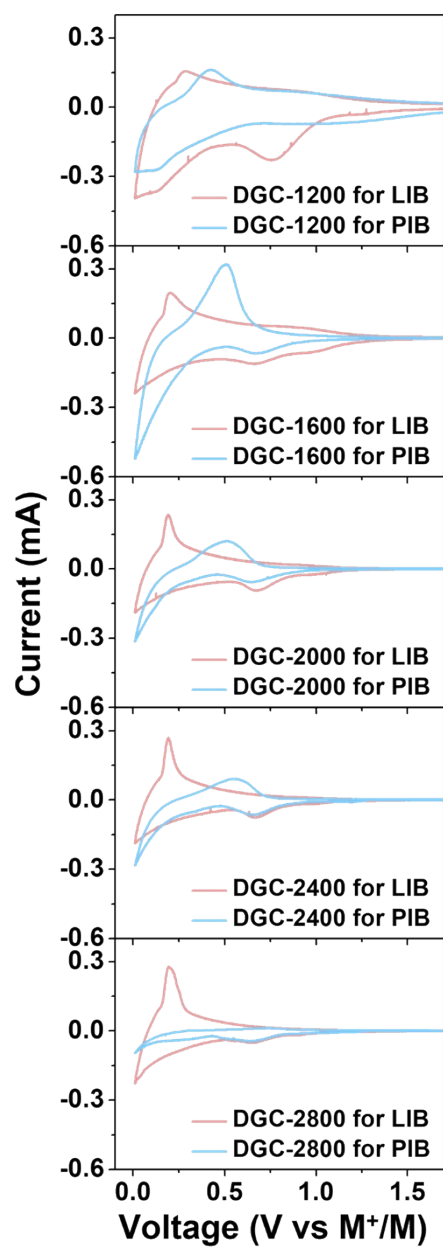


Figure S6. Cyclic voltammograms of the DGC samples for 1st cycle at a scan rate of 0.1 mV s⁻¹ in the different alkali cation charge carriers.

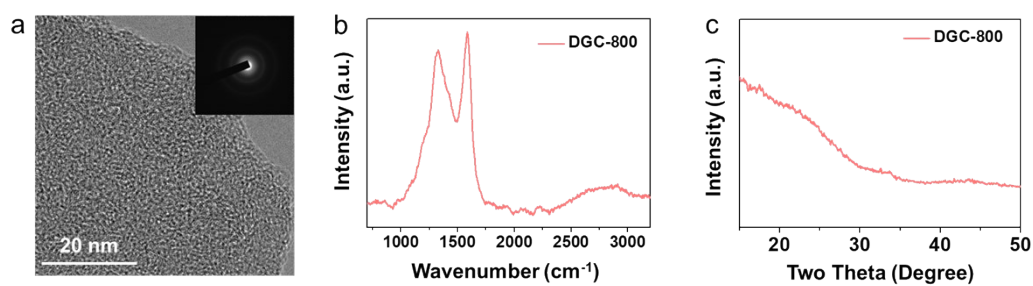


Figure S7. (a) FE-TEM image, (b) Raman spectrum, and (c) XRD pattern of the DGC-800.

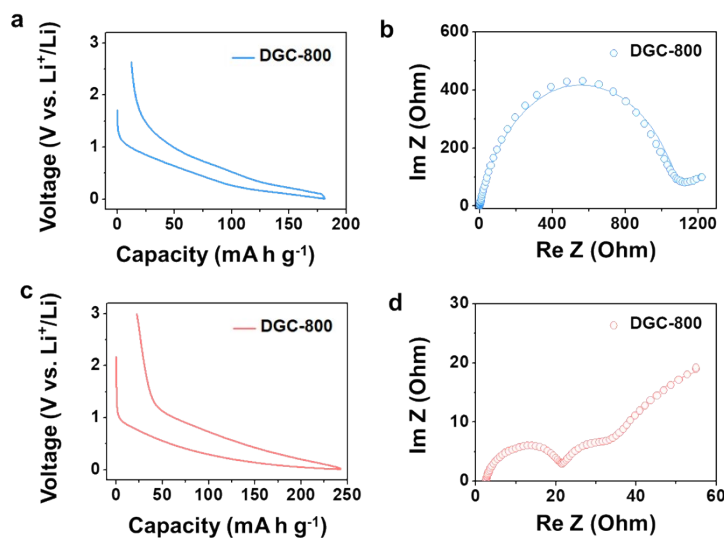


Figure S8. Galvanostatic discharge/charge profiles of the DGC-800 in (a) potassium ion and (c) lithium ion systems at a current density of 20 mA g^{-1} . EIS profiles of (b) potassiated and (d) lithiated DGC-800 samples obtained after 10th cycle.

The amorphous carbon microstructure of the DGC-800 led to a lower reversible potassium ion storage capacity of $\sim 170 \text{ mA h g}^{-1}$ (Fig. S8a). However, EIS profile of the DGC-800 reveals the similar semicircle to them of the DGC-1200 and DGC-1600 (Fig. S8b and Fig. 2i). This result suggests that the relatively low potassium ion storage capacity of the DGC-800 is due to its smaller active sites, not kinetic effects. In contrast, a reversible lithium ion storage capacity ($\sim 220 \text{ mA h g}^{-1}$) of the DGC-800 is higher than those of other DGC series samples (Fig. S8c), and its EIS profile shows lower R_f and R_{ct} values in all the tested samples (Fig. S8d and Fig. 2h). Hence, the lithium ion storage behavior of the DGC-800 is distinctive from its potassium ion storage manner, and the difference is induced by its dissimilar redox behaviors with different alkali cations. In the DGC-800 sample which has amorphous carbon microstructure with much higher d -spacing, more lithium ions can be stored by chemisorption, while the potassium ion chemisorption capacity is slight lower than the lithium ion chemisorption capacity.

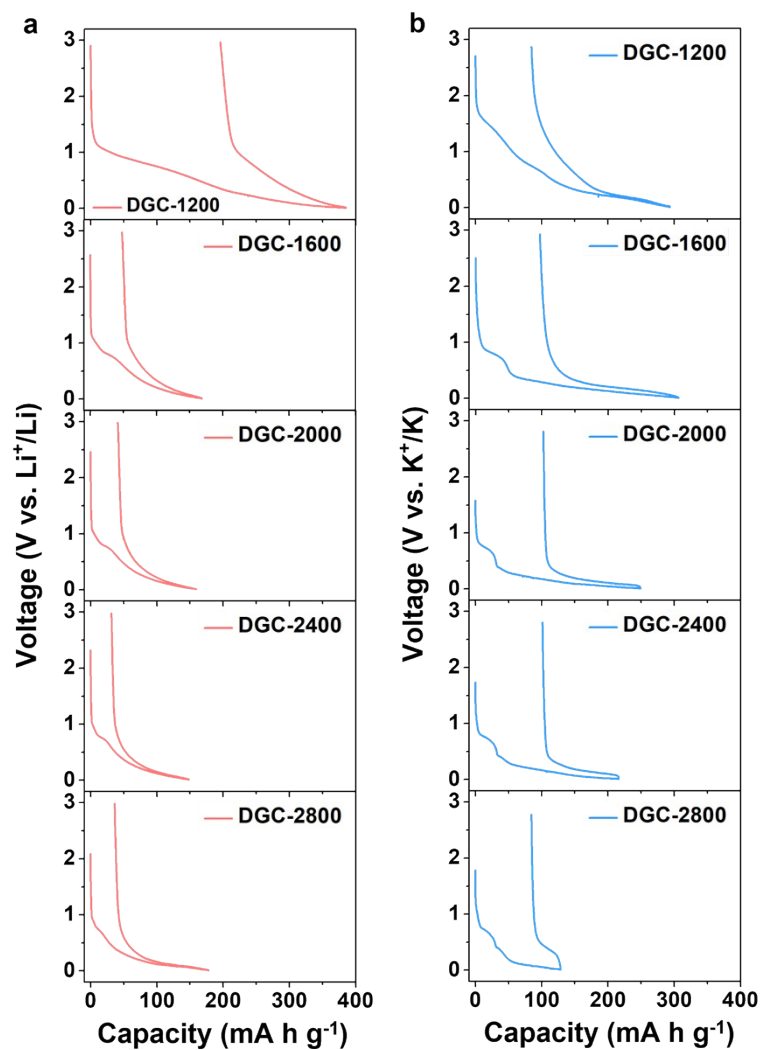


Figure S9. Galvanostatic discharge/charge profiles of the DGC samples for 1st cycle over a voltage window of 0.01-3.0 V vs. M⁺/M in electrolytes of (a) 1.0 M LiPF₆ and (b) 0.8 M KPF₆ dissolved in EC/DMC mixture solution (1:1 v/v) in a current density of 20 mA h g⁻¹.

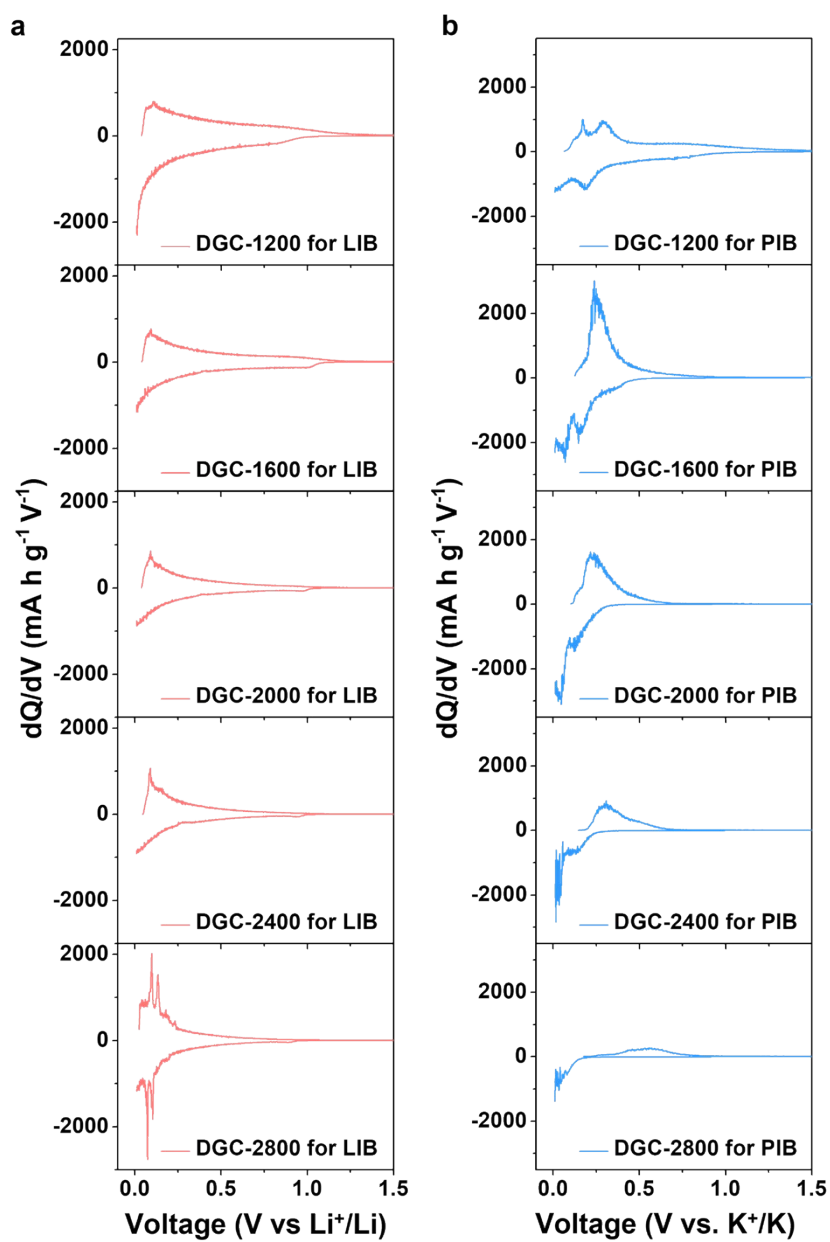


Figure S10. dQ/dV profiles of the DGC samples for 2nd cycle over a voltage window of 0.01-3.0 V vs. M^+/M in electrolytes of (a) 1.0 M LiPF_6 and (b) 0.8 M KPF_6 dissolved in EC/DMC mixture solution (1:1 v/v) in a current density of 20 mA h g^{-1} .

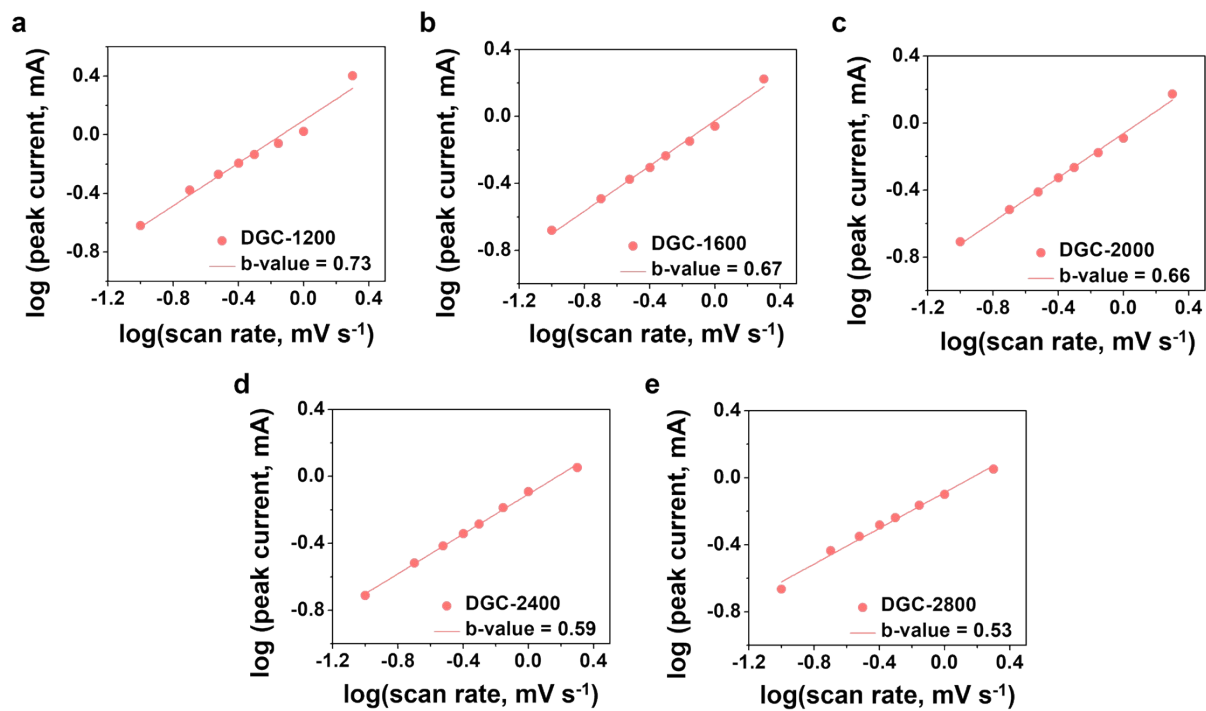


Figure S11. The Li-ion *b*-value plots of the DGC samples calculated by the cathodic peak currents of cyclic voltammograms characterized at different scan rates.

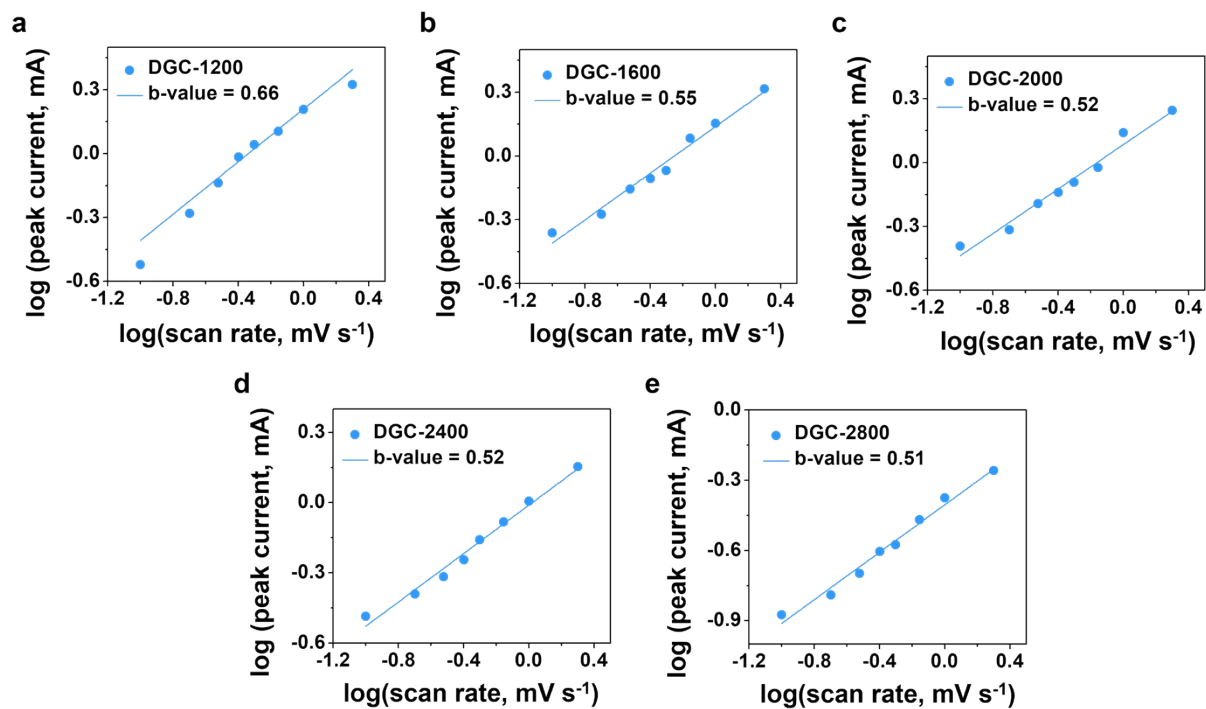


Figure S12. The K-ion b -value plots of the DGC samples calculated by the cathodic peak currents of cyclic voltammograms characterized at different scan rates.

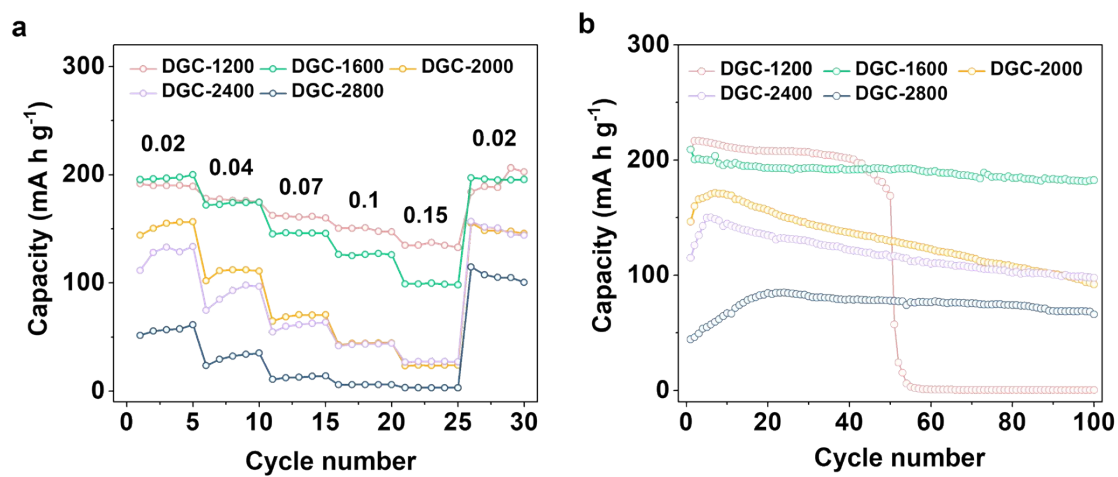


Figure S13. (a) Rate capabilities and (b) cycling performances of the DGC samples.

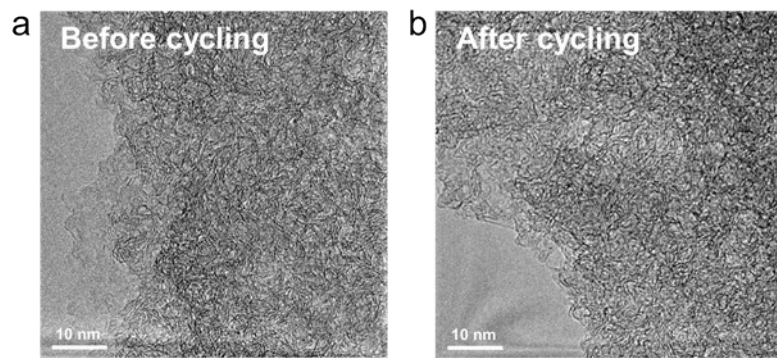


Figure S14. HRTEM images of (a) pristine DGC-1600 and (b) ex situ DGC-1600 after 10th cycle.

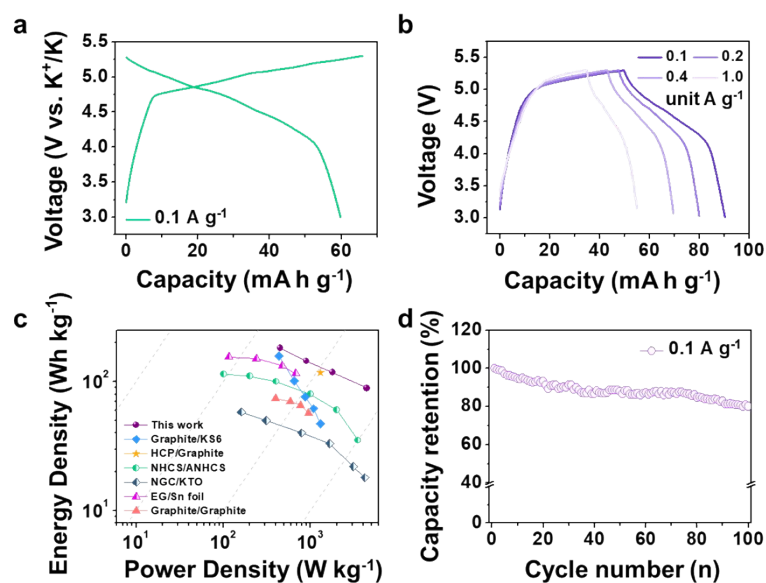


Figure S15. Electrochemical performances of the DGC-1600/NGC full cells in an electrolyte of 0.8 M KPF₆ dissolved in a 1:1 v/v mixed solution of EC/DMC over a voltage window of 3.0–5.3 V vs. K⁺/K. (a) Galvanostatic charge/discharge profiles of the NGC at 0.1 A g⁻¹, (b) Galvanostatic charge/discharge profiles of the DGC-1600/NGC full cells at different current densities. (c) Ragone plots of several potassium ion storage devices including the DGC-1600/NGC full cells. (d) Cycling performances of the DGC-1600/NGC full cells over 100 cycles.

Table S1. Textural properties of the DGC samples.

Sample name	d₀₀₂ (Å)	L_c (nm)	Integrated I_D/I_G	L_a (nm)	BET surface area (m²g⁻¹)	Average pore width (nm)	C/O ratio
DGC-1200	3.85	1.05	2.27	2.07	182.91	6.22	18.57
DGC-1600	3.67 / 3.56	1.36 / 11.56	1.91	2.46	44.25	5.77	34.46
DGC-2000	3.51 / 3.48	1.97 / 24.74	1.39	3.39	28.63	5.92	64.79
DGC-2400	3.49 / 3.43	2.61 / 34.60	0.18	25.69	23.83	5.98	110.11
DGC-2800	3.46 / 3.41 / 3.36	4.20 / 17.30 / 28.80	0.03	151.20	21.00	5.57	128.87

Table S2. Electrical conductivities of the lithiated/potassiated DGC samples.

Sample Name	Charge Carrier	Electrical Conductivity (S/cm)		
		Before Cycling	Potassiation or Lithiation	Depotassiation or Delithiation
DGC-1200	K ⁺	9.26×10^0	8.64×10^1	9.79×10^0
DGC-1600		3.74×10^1	4.26×10^2	3.27×10^1
DGC-2000		6.88×10^1	4.54×10^2	6.91×10^1
DGC-2400		8.83×10^1	4.38×10^2	8.79×10^1
DGC-2800		1.52×10^2	4.31×10^2	1.64×10^2
DGC-1200	Li ⁺	9.71×10^0	9.89×10^0	9.76×10^0
DGC-1600		3.18×10^1	3.03×10^1	3.50×10^1
DGC-2000		6.34×10^1	9.88×10^1	6.47×10^1
DGC-2400		9.03×10^1	1.04×10^2	9.32×10^1
DGC-2800		1.62×10^2	4.13×10^2	1.58×10^2

Table S3. Comparison data of the previously reported DGC materials on potassium-ion storage performances.

DGC material	Electrolyte	Initial CE	Cyclability	d_{002} (Å)	Ref.
E-carbon	0.8 M KPF ₆ in EC:EMC (1:1 v:v)	49.8%	48.5% after 430 cycles	4.10	6
HGC	0.8 M KPF ₆ in EC:DEC (1:1 v:v)	26.0%	90.0% after 200 cycles	3.41	50
NCSCNT	0.8 M KPF ₆ in EC:DEC (1:1 v:v)	14.2%	73.1% after 100 cycles	3.47	51
HCS	0.8 M KPF ₆ in EC:DEC (1:1 v:v)	61.8%	83.0% after 100 cycles	4.00	52
CNF-1250	1.0 M KPF ₆ in EC:DMC (1:1 v:v)	53.0%	94.2% after 200 cycles	3.67	53
SSAC	0.8 M KPF ₆ in EC:DEC (1:1 v:v)	51.6%	80.0% after 90 cycles	3.86	54
SC700	1.0 M KPF ₆ in EC:DEC (1:1 v:v)	62.0%	56.0% after 100 cycles	3.67	55
NCF-700	0.8 M KPF ₆ in EC:DEC (1:1 v:v)	37.8%	89.6% after 100 cycles	3.87	56
M700	0.8 M KPF ₆ in EC:DEC (1:1 v:v)	51.2%	66.7% after 100 cycles	4.04	57
NOHPHC	1.0 M KPF ₆ in EC:DMC (1:1 v:v)	25.0%	76.1% after 100 cycles	3.91	58
DGC-1600	0.8 M KPF ₆ in EC:DMC (1:1 v:v)	68.3%	87.3% after 100 cycles	3.67	This work